

## **Effect of Metallic Bath Contaminants On Zn-Ni Electroplated Alloy Properties**

*Eric Vignola & Richard Menini, Industrial Materials Institute, NRC, Boucherville, Quebec, Canada; & George Petrescu & Lucian Gurban, Ultraspec Finishing Inc., Ville St-Laurent, Quebec, Canada*

Due to hazards associated with chemicals used in cadmium and cyanide processes, replacement of cadmium coatings by Zn-Ni alloys for corrosion resistance has led to numerous studies. Optimal corrosion resistance has been reported for Zn alloys containing 5-15% in Ni, depending on the process. Even though the benefits of zinc-nickel electroplates are well documented, influence of solution contamination has not been addressed. This paper reports artificial ageing of an alkaline Zn-Ni plating bath with Pb, Cr and Cu and its detrimental effects on adhesion, throwing power, and, to a lesser extent, corrosion resistance.

**For more information, contact:**

Dr. Eric Vignola  
75 de Mortagne blvd.  
Boucherville, Quebec, Canada  
J4B 6Y4  
Phone – (450) 641-5380  
Fax – (450) 641-5105  
Email : [Eric.Vignola@cnrc-nrc.gc.ca](mailto:Eric.Vignola@cnrc-nrc.gc.ca)

## Introduction

A large segment of electroplating activities are oriented in the aerospace sector. In order to comply with stricter environmental regulations and answer customer demands towards more environmentally friendly plating processes that meet their specifications, manufacturing companies in this area are seeking a substitute for their cadmium plating lines. Promising alternatives consist of zinc-nickel alloy electrodeposits. Numerous studies on Zn-Ni plating properties like its corrosion resistance<sup>1-4</sup>, adhesion<sup>5</sup>, hydrogen embrittlement resistance<sup>4,6,7</sup>, fatigue<sup>8</sup> as well as lubricity<sup>1,3,5</sup> are reported in the literature and this, for several types of baths: acid, neutral, alkaline and other proprietary additives. In fact, depending on these processes, optimal corrosion resistance has been reported for Zn alloys containing 5-15% in Ni. Even though the benefits of zinc-nickel electroplates are well documented, influence of metallic solution contamination has not been addressed. As far as pure zinc coatings are concerned, bath contamination is a very important issue: the zinc coating aspect can drastically change in the presence of small amounts of copper (> 10 ppm) or lead (> 2 ppm) in the plating bath<sup>9</sup>. In fact, metallic contaminants ad-atoms more electropositive than zinc (Cu, Fe, Ni and Co) change the microstructure of zinc coatings<sup>10</sup>. The latter can also evolve from a bright deposit to a gray or a dark one or even change the macrostructure from a smooth to a spongy one. This can be explained by the fact that such ad-atoms electrocatalyze the competitive hydrogen evolution reaction. Other authors<sup>11</sup> showed that Pb impurities during zinc plating could lead to drastic changes in the zinc microstructure.

The main goal of this paper is to study corrosion, throwing power (TP) and adhesion properties of a Zn-Ni electrodeposit as the bath ages. These three characteristics could be greatly affected in the presence of metallic impurities coming from the working conditions (Pb from masks and Cu from bus bars) or from the substrate to be plated, e.g. high strength steels (Cr). Hence, this work reports the artificial ageing of an alkaline Zn-Ni electroplating bath with Pb, Cr and Cu salts, and its effects on properties such as adhesion, throwing power and corrosion resistance.

## Experimental

### *Substrates, plating solutions and plating procedure*

Prior to plating, Aerospace High Strength Steel plates EF-4130\* substrates (as per MIL-S-18729) were degreased in an alkaline cleaner for 5 minutes at 50°C (132°F), pickled in 50% HCl (aq) for 2 minutes at room temperature and dipped for 2 minutes in a 75 g/L (10 oz/gal) NaOH (aq) solution at room temperature. The plating bath was first prepared by immersing a stainless steel basket containing zinc balls into an aqueous NaOH solution. Then, a proprietary nickel complex was added to the solution in order to adjust the nickel concentration. Table 1 gives a more detailed description of the optimal solution composition. Metallic concentrations in

---

\* Heat-treated 37 RC, Decarburization surface 77: C% 0.29; W% 0.46; P% 0.009; S% 0.008; Cr% 0.91.

the bath were verified using atomic absorption spectroscopy (AAS). Finally, proprietary organic additives were added for leveling and brightening of the deposit. Brightener content was adjusted using a Hull cell.

All electroplating and pretreatment steps were performed in 10 L (2.6 gal) polypropylene tanks. The alloy plating solution was continuously circulated and filtered at room temperature. Current density was 4.3 A/dm<sup>2</sup> (40 ASF) and anodes were bagged (polypropylene) nickel plates. The targeted Zn/Ni atomic ratio is 95/5 to 85/15 for 8 to 12 µm (320 to 480 µin.) deposits. No post-treatment steps such as chromate conversion coating were performed on the coated specimens.

*Table 1. Optimal Zn-Ni electroplating bath composition*

COMPONENTS	RANGE
Zinc (metal)	11 to 13 g/L (1.47 to 1.74 oz/gal)
Nickel (metal)	0.2 to 0.6 g/L (0.026 to 0.08 oz/gal)
Sodium hydroxide	100 to 140 g/L (13.3 to 18.7 oz/gal)

#### *Artificial ageing with metallic contaminants*

Aqueous solutions of copper and chromium nitrate were prepared and added to the plating tank according to the targeted concentrations. For the lead contamination, lead nitrate salts were directly dissolved into the bath. Targeted contaminant concentrations are described in table 2, and were chosen from specifications given by the AESF for Zn plating<sup>9</sup>.

*Table 2. Zn-Ni electroplating contamination concentrations*

CONTAMINANTS	CONCENTRATIONS (ppm)
Pb	5, 10, 15, 20
Cr	5, 10, 15, 20
Cu	5, 30, 70, 100

#### *Adhesion testing*

The influence of contaminants on adhesion of the Zn-Ni coatings was characterized by two different tests: tape test and bend test.

The tape test was performed in accordance with ASTM D 3359-97 standard testing method, using a fine-blade cross-hatcher (11 blades, 1.0 mm spacing) with 25 mm Permaceel 99 tape. The tests were performed on two different spots of the coating.

The bend test was performed in accordance with the ASTM B 571-97 standard testing method, using a mandrel with a diameter equal to four times the thickness of the substrate. The samples were bent to a 180° angle, returned back to their initial position and examined at 10X magnification for evidence of separation or peeling of the coating.

#### *Electrochemical corrosion evaluation*

The electrochemical experiments were conducted in an aerated and magnetically stirred 3.5 % NaCl aqueous solution at 25°C according to ASTM G3-89. A flat electrochemical cell from EG&G Princeton Applied Research was used with a platinum grid auxiliary electrode and a saturated calomel reference electrode (SCE). All potentials quoted in this report are with reference to the SCE. The electrochemical measurements were taken by a computer controlled EG&G Princeton Applied Research model 273A or 263A potentiostat/galvanostat. The exposed surface area of the sample was 1 cm<sup>2</sup> and a special Teflon gasket was used for sealing and to avoid rim corrosion. At the end of each experiment the sample was cleaned with acetone and water.

For Tafel plots, corrosion potentials ( $E_{\text{corr}}$ ) were measured after 2 hours, during which the stabilization was reached. Thereafter, the potential was swept within a window of  $\pm 100$  mV with respect to the stabilization potential at a scan rate of 0.05 mV/s. Corrosion current densities ( $j_o$ ) were calculated from the polarization curves (overpotential ( $\eta$ ) versus logarithm of the current density ( $\log j$ )).

Regarding the cyclic voltammetry curves, samples were conditioned for 5 minutes at a potential of ~300 mV more cathodic than the corrosion potential. Subsequently, the potential was scanned at 5 mV/s in the anodic direction to determine the anodic activity of the different studied coatings and their ability to passivate. Following that scan, a cathodic sweep up to the initial potential was recorded to determine if a stable oxide film covered the sample.

#### *Throwing power and chemical uniformity*

Assessment of throwing power ( $TP$ ) was made with the Haring-Blum cell. This cell consists of a mobile anode at the center of the cell, while two cathodes are located at opposite ends at a relative distance from the anode. Figure 1 illustrates the Haring-Blum cell with the dimensions used for the experiments.

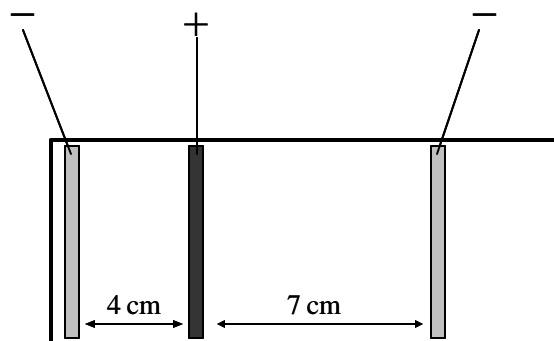


Fig. 1. Haring Blum cell

This geometry allows determination of the throwing power by measuring the ratio  $R$  (near-to-far) of weights deposited on the cathodes. Knowing the ratio  $L$  of the far-to-near cathode-anode distance, one can calculate the throwing power of the plating system using the Field equation (1).

$$TP (\%) = 100 \times \frac{(L - R)}{(L + R - 2)} \quad (1)$$

Throwing power was studied on the most contaminated solutions (Zn-Ni / Pb 20 ppm, Zn-Ni / Cr 20 ppm and Zn-Ni / Cu 100 ppm) and compared with the pure Zn-Ni coating. This was done at room temperature during 15 minutes at 2 A with a nickel counter electrode. Zincated iron Hull cell plates were used as cathodes. The zinc coating was removed by dipping the plates into 10 % v/v aqueous HCl until they became bright and clear of smut. Before and after plating, plates were rinsed with DI water, rubbed off with a clean cloth, dehydrated with a heat gun and weights measured to the fourth decimal.

A bent cathode plating technique was used to evaluate the consistency of Zn and Ni concentration distribution over the surface of the coating. According to the recommendation of the JG-PP Protocol<sup>1,2</sup>, X-ray fluorescence (XRF) at a step of 2,500 counts per second (cps) was used for Zn and Ni during 100 seconds. The intensity of fluorescent current was 0.7 nA. Measurements were performed at two different spots, each one having a 250  $\mu$ m (10 mil) radius, at three different locations determined according to their distance from the anode. Cell configuration is shown in figure 2, and consists of a typical Hull cell containing a nickel anode and a steel cathode as used in Hull cell testing. Encircled areas 1, 2 and 3 in figure 2 represent the three different regions analyzed by XRF. The cathode was bent at a 90 degrees angle. Open edges and the closed bend are located at 4.5 (0.18 in.) and 7.5 cm (0.30 in.) from the anode, respectively.

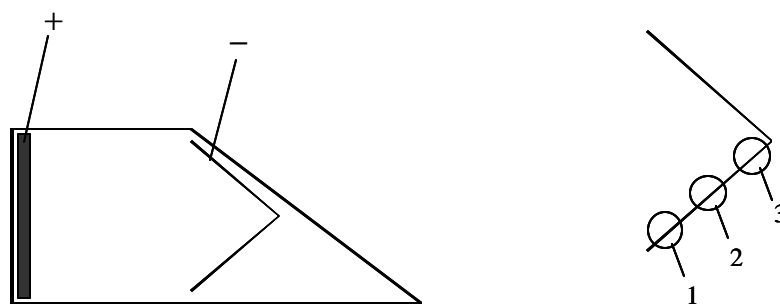


Fig.2. Bent cathode testing

## Results

### *Coating composition*

All the Zn-Ni electrodeposited alloy coatings described in figure 3 were silvery bright, even though plated specimens were slightly yellow with Cu and slightly darker with Pb contaminants than with pure Zn-Ni. When Cr was present, coatings were brighter than pure Zn-Ni itself. As indicated by a solution makeup provider, all nickel percentages were kept between 5 and 11 % to ensure maximum corrosion resistance.

Table 3 compares the contaminant concentrations in the bath solution before and after plating. It can be assumed that the decrease of metallic contaminants concentration in the bath after plating corresponds to their incorporation into the Zn-Ni coatings, since this could not be verified by XRF (detection limits are approximately 1 %). In this case, consumption of contaminant is more important for Cu, where approximately 65 to 80 % of the initial contaminant solution content is consumed. Consumption of Cr is between 50 to 60%, while Pb shows the lowest consumption: values are in the range of 20 to 30 %. These discrepancies are due to the higher plating efficiency of Cu compared to Cr and Pb, as well as low Pb salt solubility.

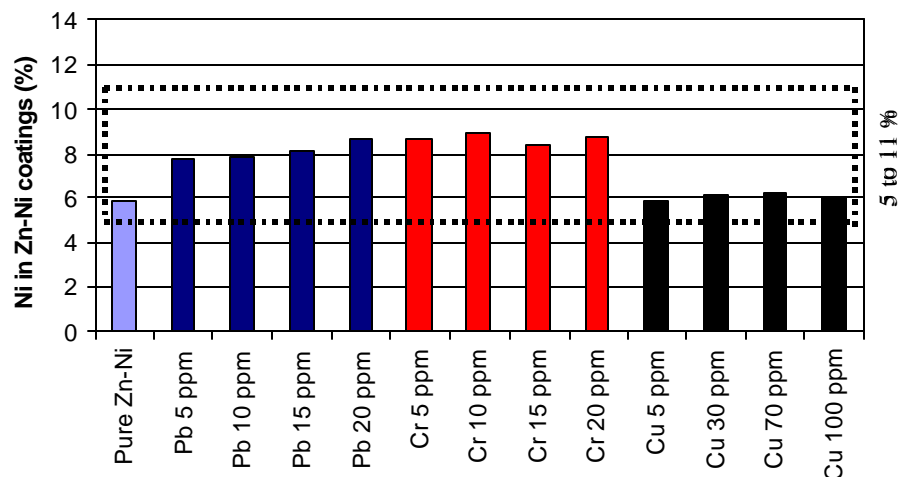


Fig.3. Ni concentrations in Zn-Ni coatings

Table 3 - Residual metallic contaminants in the bath after Zn-Ni plating

CONTAMINANT	DETECTION LIMIT (ppm)	CONCENTRATION (ppm)			
		FINAL [INITIAL]			
Pb	0.02	5.3 [5]	8.3 [10]	12 [15]	14 [20]
Cr	0.01	1.9 [5]	3.7 [10]	6.7 [15]	10 [20]
Cu	0.01	-- [5]	6.5 [30]	-- [70]	36 [100]

### Adhesion

Adhesion of the Zn-Ni coating exhibits a 5B result according to the tape test ASTM D 3359-97, for which classification is made as described in appendix I.

A gradual reduction of adhesion (3B and 4B) is observed until a 15 ppm concentration is reached for the Pb contaminant. However, a 20 ppm Pb contamination exhibits good adhesion properties, comparable to those of the pure Zn-Ni system. On the other hand, when doped with small amounts of Cr, the Zn-Ni coating undergoes a more definite loss of adhesion, starting from 5B with 5 ppm to 1B with 20 ppm. A similar trend applies for the Cu contaminated system, showing a noticeable decrease in adhesion, starting at 3B with 5 ppm going down to 1B with 100 ppm. It is not clear why the 70 ppm concentration is giving a classification 5B as results; experimental error is likely the cause. Tests were repeated twice per coating to address reproducibility and results are compiled in table 4. As an overview, the magnitude of the reduction effect of Pb, Cr and Cu respectively on adhesion from the tape test follows the trend:

$$\text{Cu} > \text{Cr} > \text{Pb}$$

The bend test offers an alternative for the characterization of adhesion. According to ASTM B 571-97, the coating passes the adhesion test if no material removal is observed

following a 180° bend. Classification was made as Y (yes) if the coating stayed intact or as N (no) if the coating did not stay intact and delamination or spalling from the substrate occurred. In this regard, table 4 also shows the results obtained by the bend test, and it clearly demonstrates that only pure Zn-Ni exhibits satisfactory (Y) substrate adhesion. In fact, all Zn-Ni coatings containing Pb, Cr or Cu respectively produced spalling upon bending. It was also visually observed that the intensity of spalling increased with increasing contaminant concentrations.

Table 4 – Adhesion of Zn-Ni coatings influenced by Pb, Cr and Cu contaminations, respectively

CONTAMINANT	TAPE TEST #1	TAPE TEST #2	BEND TEST
Pure Zn-Ni	5B	5B	Y
Pb (5 ppm)	4B	4B	N
Pb (10 ppm)	3B	4B	N
Pb (15 ppm)	3B	4B	N
Pb (20 ppm)	5B	5B	N
Cr (5 ppm)	4B	5B	N
Cr (10 ppm)	2B	2B	N
Cr (15 ppm)	1B	1B	N
Cr (20 ppm)	1B	1B	N
Cu (5 ppm)	3B	3B	N
Cu (30 ppm)	1B	1B	N
Cu (70 ppm)	5B	5B	N
Cu (100 ppm)	1B	1B	N

### Electrochemical corrosion

Corrosion testing in the aeronautic sector is usually performed by salt spray (ASTM B117) on scribed and unscribed chromated specimens<sup>12</sup>. The present electrochemical study was conducted to accelerate, evaluate and comprehend possible changes in corrosion behavior of Zn-Ni coatings.

Table 5 displays the results obtained for the electrochemical corrosion evaluation ( $E_{\text{corr}}$  and  $j_o$ ) of the coatings containing the three contaminants at four different concentrations. To give a better view of these results, the rate of dissolution ( $h$ ) in mil per year (mpy) was calculated using equation (2)<sup>13</sup>, where  $i_o$  is the corrosion current,  $t$  the exposure time,  $M_{\text{Zn-Ni}}$  the molar mass,  $\rho$  the density and  $r$  the radius of the exposed surface.

$$h = \frac{i_o t M_{\text{Zn-Ni}}}{\rho r^2 n F} \quad (2)$$

As expected, pure Zn-Ni coating exhibits high corrosion resistance in such media (3.5 % NaCl). In this case,  $j_o$  value is estimated at 13.0  $\mu\text{A}/\text{cm}^2$  corresponding to a 2.4 mils per year dissolution rate, which is, according to Fontana<sup>13</sup>, classified as “*Excellent*” in terms of corrosion resistance (1-5 mpy bracket). The other two nearby brackets in this classification are: “*Outstanding*” (<1 mpy) and “*Good*” (5-20 mpy). Bath contamination by Cu and Pb slightly



decreases the corrosion resistance of Zn-Ni coatings at concentrations superior to 30 and 5 ppm, respectively. However, corrosion resistance for Zn-Ni coatings obtained with Cr contaminations are difficult to assess since the  $j_o$  or  $h$  values are either classified as “*Excellent*” (for the 10 and 20 ppm concentrations) or as “*Good*” (for 5 and 15 ppm concentrations), thus independently of the Cr concentration. Nonetheless, it must be pointed out that all high  $h$  values for Cr (7.4 and 7.8 mpy) have also high standard deviation values (5.7 and 2.1 respectively). As far as corrosion potentials are concerned, Cu contamination tends to slightly decrease the corrosion resistance of Zn-Ni coatings:

$$E_{\text{corr}}(\text{Cu}) < E_{\text{corr}}(\text{pure Zn-Ni})$$

Regarding the  $E_{\text{corr}}$  values obtained for Pb and Cr electrolyte contaminations, no clear conclusions could be drawn since all values are close (see the standard deviation data) to -982 mV, obtained with the pure Zn-Ni coating.

*Table 5 – Corrosion electrochemical assessment of Zn-Ni coatings in 3.5% NaCl*

CONTAMINANT	$E_{\text{corr}}$		$j_o$		$h$	
	mV <sub>ECS</sub>	+/-	μA/cm <sup>2</sup>	+/-	mil/year	+/-
Pure Zn-Ni	-982	2.1	13.0	3.8	2.4	0.7
Pb (5 ppm)	-987	4.2	16.4	4.5	3.0	0.8
Pb (10 ppm)	-997	4.4	33.0	9.8	6.1	1.8
Pb (15 ppm)	-989	2.6	32.5	6.0	6.0	1.1
Pb (20 ppm)	-963	4.5	33.0	6.8	6.1	1.3
Cr (5 ppm)	-990	12.5	40.1	30.7	7.4	5.7
Cr (10 ppm)	-994	8.4	16.3	3.0	3.0	0.5
Cr (15 ppm)	-977	8.1	42.2	11.1	7.8	2.1
Cr (20 ppm)	-978	8.5	9.0	3.3	1.7	0.6
Cu (5 ppm)	-993	5.7	12.4	1.4	2.3	0.3
Cu (30 ppm)	-1013	9.0	11.9	6.4	2.2	1.2
Cu (70 ppm)	-991	19.3	23.5	4.7	4.3	0.9
Cu (100 ppm)	-1002	3.5	30.2	17.4	5.6	3.2

To have a better insight on the corrosion behavior of the different Zn-Ni coatings, a study of the polarization curves recorded using the cyclic voltammetry technique was performed. Figures 4 and 5 show polarization recordings for the lowest and highest concentrations of each contaminant. This set of plots shows that even at low contaminant concentrations, the large passivation peak visible at approximately  $E = -0.6 \text{ V}_{\text{SCE}}$  for pure Zn-Ni coating (black curve) is removed. However, when the back scans are plotted, it seems that no dissolution of the oxide passive layer is observed with the three contaminants. A higher plot magnification was needed in order to check if the oxide passive layer was stable when contaminants were used. Except for the 100 ppm Cu contamination concentration, oxide layers are not completely stable since cathodic current densities between - 0.5 and - 1.5 mA/cm<sup>2</sup> are recorded during the back scans, see Figs. 4B and 5B.

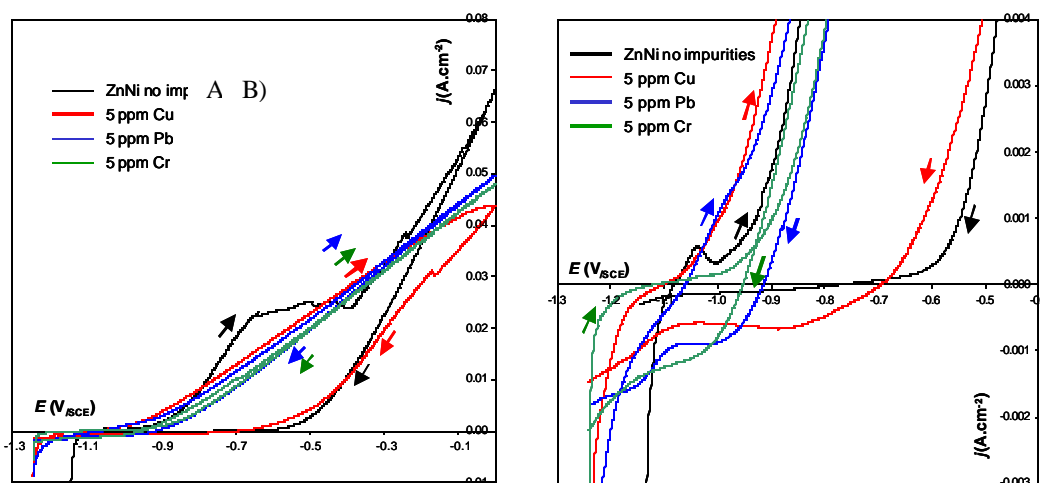


Fig. 4. Cyclic voltammetry with low contaminant concentration at low (A) and high(B) magnification

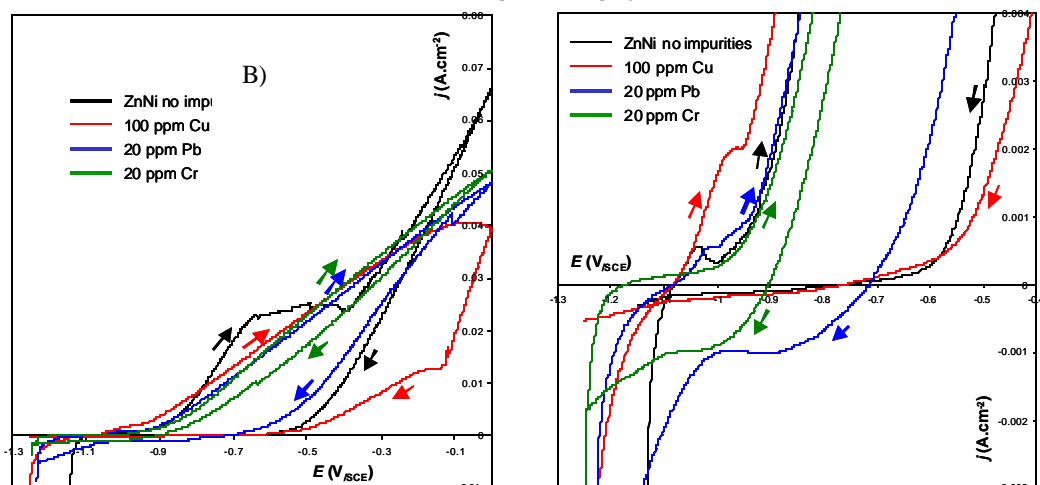


Fig. 5. Cyclic voltammetry with high contaminant concentration at low (A) and high(B) magnification

As far as the influence of increasing contaminant concentration upon the polarization recordings is concerned, it is difficult to establish a clear relationship between the contaminant concentration and the whole curve aspects or the oxide layer stability.

#### Throwing power and chemical uniformity

Evaluation of throwing power ( $TP$ ) using the Haring-Blum cell shows that  $TP$  is more important when no contaminant is present in the Zn-Ni system ( $TP = 17.2$ ) (see table 6). Pb contamination reduces the measured property, with  $TP = 11.2$ , which is about 2/3 of pure Zn-Ni value. However, the same amount of Cr in the bath reduces the throwing power ( $TP = -4.9$ ) by

as much as 128 % compared to the Zn-Ni itself, while 100 ppm of Cu alters the throwing power ( $TP = -32.6$ ) of the plating bath to a higher extent.

*Table 6 - Throwing power of Zn-Ni solutions influenced by Pb, Cr and Cu contaminants*

CONTAMINANT	R	TP <sup>a</sup> (%)	TP vs BLANK (%)
Pure Zn-Ni	1.53	17.2	0.0
Pb (20 ppm)	1.60	11.2	-35
Cr (20 ppm)	1.83	-4.9	-128
Cu (100 ppm)	2.48	-32.6	-290

<sup>a</sup> Obtained accordingly to equation (2) with  $L = 1.75$ .

In order to evaluate the influence of contaminant concentration on the alloy chemical uniformity, an elemental distribution of Zn and Ni in the coating is displayed in table 7. As we approach the inner bend of the bent cathode, the effect of contaminant concentration on the chemical composition of the coating changes. Because of variations in the current densities, table 7 shows that Ni concentration in the alloy decreases from area **1** (high current density) to **3** (low current density) in all conditions. However, decrease in Ni content becomes more important when contaminants are initially added to the plating bath. In this regard, Cu and Cr inhibit Ni plating in low current density areas more than Pb. According to the percentage change in Ni concentration from area **1** to **3** (see last row of table 7), the ability to plate Ni from the Zn-Ni alkaline bath in low current density areas is classified as follows:

pure Zn-Ni > Pb (20 ppm) > Cr (20 ppm) > Cu (100 ppm)

*Table 7 – Coating composition obtained by X-ray fluorescence at three different locations on the bent cathode.*

AREA <sup>a</sup>	ATOM	Pure Zn-Ni (atom %)	Pb (20 ppm) (atom %)	Cr (20 ppm) (atom %)	Cu (100 ppm) (atom %)
<b>1</b>	Zn	94.39	94.31	94.33	93.11
	Ni	5.61	5.61	5.61	5.65
	Pb	< 1	< 1	< 1	< 1
	Cr	< 1	< 1	< 1	< 1
	Cu	< 1	< 1	< 1	1.24
<b>2</b>	Zn	94.74	94.63	94.96	93.75
	Ni	5.27	5.37	5.04	5.09
	Pb	< 1	< 1	< 1	< 1
	Cr	< 1	< 1	< 1	< 1
	Cu	< 1	< 1	< 1	1.17
<b>3</b>	Zn	95.22	95.12	95.35	94.15
	Ni	4.78	4.75	4.64	4.67
	Pb	< 1	< 1	< 1	< 1
	Cr	< 1	< 1	< 1	< 1
	Cu	< 1	< 1	< 1	1.18
% change in Ni from area <b>1</b> to <b>3</b>		-14.8	-15.3	-17.3	-17.4

<sup>a</sup> Areas 1 and 3 are the closest and the farthest from the anode, respectively (see figure 2).

Even though variations go down to approximately -17 %, Ni concentrations are still in the range of optimal concentrations. In fact, only area **3** does not meet the optimal specification (5 to 11 % for nickel) for the alloy composition. However, it should be noted that nickel composition at areas **1** and **2** are close to 5 %, which is in the lower limit of the optimal specification. Since the maximum variation is -17.4 % for the nickel concentration, an 8 % (or higher) Ni composition for area **1** should meet the provider specification for configurations similar to the bent cathode.

## Conclusion

As far as adhesion was concerned, only pure Zn-Ni coating passed both the tape and the bend tests respectively. It should be noticed, that the bend test was part of the JG-PP test protocol on the cadmium replacement project in the aeronautic sector. Therefore Cu, Cr and Pb contamination concentrations should be carefully monitored down to 5 ppm to avoid cracking or peeling of the Zn-Ni coating.

Overall contamination of the Zn-Ni alloy bath by Cu, Pb and Cr slightly decreases the corrosion resistance of non-chromated Zn-Ni coatings. Nonetheless, for each contaminant concentration, rates of dissolution were either “*Excellent*” (1-5 mpy) or “*Good*” (5-20 mpy) according to the corrosion classification brackets. However, relatively non-stable oxides were formed on the coating surface and this was particularly true for Cr contamination concentrations > 5 ppm.

Throwing power of the Zn-Ni alloy, assessed using the Haring-Blum cell and the Field equation, showed a clear reduction when high concentrations in Pb, Cr or Cu were present in the bath. In fact, high concentrations of contaminants also lower alloy nickel content in more recessed areas compared to the pure Zn-Ni coating, as shown by the bent cathode test. However, the proper use of specially designed anodes as well as optimized nickel composition around 8 % should improve flexibility of the process.

Finally, great care must be taken during Zn-Ni bath preparation and plating operations since concentrations as low as 5 ppm of copper, lead and chromium have shown adverse effects, particularly on adhesion of Zn-Ni coatings. Plating solutions should be prepared with high purity de-ionized water to prevent supplemental contamination. Masks, bus bars, tools or whatever material containing Pb, Cr and/or Cu should not be used for the alkaline Zn-Ni process. During the electroplating process, the metallic contamination by Cu, Cr and Pb should be carefully monitored.

## References

- [1] G.F. Hsu, *Plat. & Surf. Finish.*, **4**, 52 (1984)
- [2] C.B. Hiott, *Galvano Organo Traitement de Surface*, **615**, 387 (1991)
- [3] M.D. Thomson, *Trans. IMF*, **74**(3), 3 (1996)
- [4] J.A. Bates, *Plat. & Surf. Finish.*, **4**, 38 (1994)
- [5] K.R. Baldwin and C.J.E. Smith, *Wire Industry*, Nov., 667 (1997)
- [6] D.A. Wright and N.Gage, *Trans. IMF*, **72**(4), 130 (1994)
- [7] M.J. Carr and M.J. Robinson, *Trans. IMF*, **73**(2), 58 (1995)
- [8] D.A. Wright, N.Gage and B.A. Wilson, *Plat. & Surf. Finish.*, **7**, 18 (1994)
- [9] F. Altmayer and J. Kiepora, *Zinc Plating, Electroplating & Surface Finishing*, AESF Educational Course, 2000
- [10] M.M. Jaksic, *Surf. Coat. Tech.*, **28**, 113 (1986)
- [11] D.J. Mackinnon, J.M. Brannen and R.C. Kerby, *J. Appl. Electrochem.*, **9**, 55 (1979)
- [12] Engineering and Technical Services for Joint Group on Pollution Prevention (JG-PP) Projects, Joint Test Protocol BD-P-1-1, prepared by: National Defense Center for Environmental Excellence (NDCEE), June 30, 1999.  
<http://www.jgpp.com/projects/cadmium/bisdsjtp.pdf>
- [13] M.G. Fontana, *Corrosion Engineering*, 3rd Edition, McGraw-Hill, New York, 1986, p 172.

## List of symbols

Symbol	Physical meaning	Units
$\rho$	Zn-Ni density	$\text{kg.m}^{-3}$
$\eta$	Overpotential	V
$E$	Potential	$V_{\text{SCE}}$
$E_{\text{corr}}$	Corrosion potential	$V_{\text{SCE}}$
$F$	Faraday constant	$\text{C.equiv}^{-1}$
$h$	Corrosion dissolution rate	$\text{mils.years}^{-1}$
$i$	Current	A
$i_o$	Corrosion current	A
$j$	Current density	$\text{A.cm}^{-2}$
$j_o$	Corrosion current density	$\text{A.cm}^{-2}$
$L$	Far-to-near cathode-anode distances ratio	--
$M_{\text{Zn-Ni}}$	Molecular Mass	kg
$n$	Number of electron involved	--
$R$	Near-to-far ratio of deposited weights on cathodes of the Haring Blum cell	--
$r$	Radius of exposed surface area	m
SCE	Saturated Calomel Electrode	--
$t$	Time	s
$TP$	Throwing power coefficient	%

## Appendix I

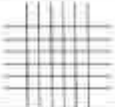
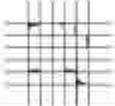
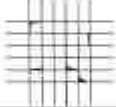

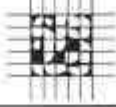
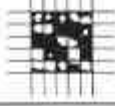
Classification of Adhesion Test Results		
Classification	Percent Area Removed	Surface of crosscut area from which flaking has occurred for six parallel cuts and adhesion range by percent
5B	0% None	
4B	Less than 5%	
3B	5-15%	
2B	15-35%	
1B	35-65%	
0B	Greater than 65%	

Fig. A-I. Classification of adhesion according to ASTM D 3359-97